

MOL #29967

TITLE PAGE

**INSIGHTS INTO THE CHOLECYSTOKININ 2 RECEPTOR BINDING SITE AND  
PROCESSES OF ACTIVATION.**

**Michaël R Paillasse<sup>1</sup>, Céline Deraeve<sup>1</sup>, Philippe de Medina, Loubna Mhamdi, Gilles  
Favre, Marc Poirot and Sandrine Silvente-Poirot<sup>2</sup>.**

**INSERM U563, Equipe : Métabolisme, Oncogénèse et différenciation cellulaire, Institut Claudius Regaud  
24 rue du Pont St-Pierre, 31052 Toulouse cedex France (CD, LM, GF, MP, SSP).**

**AFFICHEM, Institut Claudius Regaud, 24 rue du Pont St-Pierre, 31052 Toulouse cedex France (MRP,  
PDM).**

**MOL #29967**

**RUNNING TITLE PAGE**

Running title: Cholecystokinin Receptor Binding Site And Activation Processes

**Corresponding author:**

Dr Sandrine Silvente-Poirot,

INSERM U563, Equipe : Métabolisme, Oncogénèse et différenciation cellulaire,

Institut Claudius Regaud

20-24 rue du Pont Saint Pierre, 31052 Toulouse Cedex, France

Tel : 33 5 61 42 46 48 ; Fax : 33 5 61 42 46 31

Email : poirot.sandrine@ claudiusregaud.fr

Abstract: 248 words

Running title: 56 characters

Introduction: 735

Discussion: 1624

Number of the text pages: 36

Number of the tables: 3

Number of the figures: 5

Number of the references: 37

**ABBREVIATIONS:**

CCK, cholecystokinin; CCK-9s, sulphated CCK nonapeptide; CCK2R, cholecystokinin receptor type 2; extracellular loop, ECL; ICL, intracellular loop; wild type, WT; transmembrane, TM; GPCR, G protein-coupled receptor; IP, inositol phosphate.

## ABSTRACT

The cholecystokinin 2 receptor (CCK2R) appears as a pharmacological target for the treatment of many major diseases. To complete the mapping of the CCK2R binding site and its activation processes, we have looked for the receptor residues that interact with Trp<sup>6</sup>, an essential residue for CCK binding and activity. In the molecular model of the CCK-occupied CCK2R that we built, the indole group of Trp<sup>6</sup> stacked with the phenyl ring of Phe120 (ECL1) and interacted with the imidazole group of His381(H7.39) and the phenyl ring of Tyr385(H7.43). Mutagenesis and pharmacological studies validated these interactions. Importantly, the mutation of Phe120 to Trp conferred constitutive activity to the CCK2R. Molecular modeling and experimental works identified the residues involved in the activation cascade initiated by Trp<sup>6</sup> and revealed that the constitutively active F120W mutation mimics the conformational changes induced by Trp<sup>6</sup> resulting in : i) the exposure of Glu151(E3.49) of the conserved E/DRY motif ii) the formation of an amphiphatic pocket involving protonated Glu151(E3.49) and Leu330 (ICL3) iii) the opening of the intracellular loops 2 and 3 and the release of Arg158 (ICL2). The R158A mutation was shown to affect inositol phosphate production while the E151A and L330E mutations induced constitutive inositol phosphate production. Given that a constitutively active variant of the CCK2R has been identified in different cancers and the fact that the E151A mutant has been reported to induce tumours, these studies should help in the development of potent inverse agonists to inhibit the constitutive activation of the CCK2R.

## INTRODUCTION

The cholecystokinin 2 is a member of the rhodopsin-like G protein-coupled receptor family that mediates important physiological functions by binding cholecystokinin (CCK) and gastrin peptides. The CCK2R is present in the central nervous system where it regulates anxiety/panic attacks, dopamine release and nociception. In the periphery, it regulates acid, histamine and leptin secretion as well as cell growth and differentiation (Aly et al., 2004; Rozengurt and Walsh, 2001; Wank, 1995). It is also expressed in different cancers of neuroendocrine origin whereas it is not present in the corresponding normal tissues (Reubi et al., 1997). In different human cancers, a variant of this receptor that displays constitutive cell proliferation and PLC activation has been isolated (Ding et al., 2002; Harris et al., 2004; Hellmich et al., 2000), indicating that permanent activation of these receptors may have pathological consequences. We have reported a link between the constitutive activation of the CCK2R and the development of tumors by showing that the mutation of the residue E151 to Ala of the highly conserved E/DRY motif induces ligand-independent receptor activation as well as tumor formation (Gales et al., 2003b). Given the clinical importance of CCK2R-mediated functions, great interest has been devoted to the identification of efficient and selective CCK2 ligands (de Tullio et al., 2000). However to date none of these compounds have been used as a therapeutic agent, highlighting the need to better understand the structural basis of ligand-receptor interactions and activation, to rationalize the synthesis of CCK ligands. To this end, we have started several years ago to characterize residues involved in the rat CCK2R binding site and PLC activation, one of the main signaling pathways activated by the CCK2R after its coupling to Gq proteins (Gales et al., 2000; Gales et al., 2003a; Gales et al., 2003b; Silvente-Poirot et al., 1999; Silvente-Poirot et al., 1998; Silvente-Poirot and Wank,

1996). The CCK peptide exists physiologically in multiple forms processed from a 115-amino acid preprohormone. The C-terminal amidated tetrapeptide of CCK represents the minimal peptide that present nanomolar affinity and activity for the CCK2R.

We first showed that the extracellular loops (ECL) 1 and 2 were involved in CCK binding and activity by mutagenesis studies (Silvente-Poirot et al., 1998). We then demonstrated that His207 in ECL2 of the CCK2R interacts directly with the C-terminal Asp<sup>8</sup> of CCK (Silvente-Poirot et al., 1999). Based on these different results, we established a molecular model of the CCK2R occupied by CCK. This model enabled us to identify two new residues not identified by mutagenesis, Tyr189(Y4.60) and Asn358(N6.55), in interaction with the C-terminal Phe<sup>9</sup>-amide of CCK (Gales et al., 2003a). Mutagenesis of these residues and affinity studies with modified peptides allowed us to confirm these interactions and to show the involvement of the transmembrane domains (TM) 4 and 6, in addition to the ECL2 in the CCK binding site and receptor activation. Similar residues in TM4 and TM6 were reported as important for CCK binding in the human CCK2R (Blaker et al., 1998; Ren et al., 2003). While TM6 domain has been shown to be important for GPCRs of the rhodopsin family and the CCK2R activation (Gether, 2000; Schwartz et al., 2006), the TM4 domain has received much less attention. However cross-linking studies of rhodopsin with a photoactivated chromophore labelled a residue in TM4 and indicated that a substantial movement of TM3 and TM4 accompany receptor activation (Borhan et al., 2000). In addition, residues in TM4 and ECL2 in the dopamine D2 receptor have been shown to form the binding site crevice (Javitch et al., 2000; Shi and Javitch, 2004). Mutational data also indicated that ECL2 is important for the stability of the retinal binding site in rhodopsin and meta II (Doi et al., 1990). Several other reports implicated ECL2 in ligand specificity in aminergic and other small ligands (Shi and Javitch, 2002). Interestingly, in our molecular model, the ECL2 enters

**MOL #29967**

into the cavity formed by the seven helices, as observed for rhodopsin in the X-ray structure, to interact with the C-terminal part of CCK (Gales et al., 2003a; Silvente-Poirot et al., 1999). The fact that our molecular model and experimental data are in accordance with these data push us to pursue the characterization of the CCK binding site. When we evaluated the contribution of each amino acid of CCK2-9 peptide to bind and activate the WT-CCK2R, we found that the exchange of Trp<sup>6</sup> to Ala induced the greatest decrease on binding and IP production (Silvente-Poirot et al., 1999). The present study was undertaken to define the amino acids of the receptor in interaction with Trp<sup>6</sup> of the ligand and to explore the contribution of this residue in receptor activation.

## MATERIALS AND METHODS

**Material** - The sulfated C-terminal nonapeptide of CCK [Thr<sup>28</sup>, Nle<sup>31</sup>]-CCK25-33 was synthesized as described previously and referred to as CCK-9s (Gales et al., 2003b). <sup>125</sup>I-Na (2000 Ci/mMole) was from Amersham, Les Ulis, France. (Thr<sup>28</sup>, Nle<sup>31</sup>)-CCK25-33 was conjugated with the Bolton-Hunter reagent, purified and radioiodinated as described previously and referred to as <sup>125</sup>I-BH-CCK-9s (Gales et al., 2003b). The compound RPR048 (2-{3-[3-((3-Methoxy-phenyl)-[(methyl-phenyl-carbamoyl)-methyl]-carbamoyl)-methyl]-ureido]-phenyl}-propionic acid), kindly provided by Sanofi-Aventis (France), was previously characterized as an inverse agonist of the CCK2R (Gales et al., 2003b).

**Construction of mutant Receptor cDNAs** - Mutant receptor cDNAs were constructed by oligonucleotide-directed mutagenesis (QuickChange™ Site-directed Mutagenesis Kit, Stratagene, France), using rat CCK2R cDNAs as template. Mutations were confirmed by DNA sequencing using an automated sequencer (Applied Biosystems).

**Transfection of Wild Type and Mutant Receptor cDNAs into Mammalian Cells** - COS-7 cells were grown in Dulbecco's modified Eagle's medium (DMEM) supplemented with 5 % fetal calf serum. Usually, 2 micrograms of the CCK2R and mutant receptor cDNAs subcloned in pCDL-SRα were transiently transfected into COS-7 cells using the DEAE/Dextran method as described previously (Silvente-Poirot and Wank, 1996). Twenty four hours after transfection, the transfected cells were transferred to 24-wells culture plates and seeded at a density of approximately  $1 \times 10^5$  cells/well and assayed for <sup>125</sup>I-BH-CCK-9 binding or inositol phosphate (IP) hydrolysis.

Binding of  $^{125}\text{I}$ -BH-CCK-9 to transfected COS-7 Cells - Twenty four hours after the transfer of transfected cells to 24-well plates, the cells were washed once with cold phosphate-buffered saline (PBS), pH 7.4 containing 0.1% bovine serum albumin (BSA) and incubated in DMEM containing 0.1 % BSA for 60 min at 37° C with 50 pM of  $^{125}\text{I}$ -BH-CCK-9 with or without increasing concentrations of unlabelled peptides. Cell associated  $^{125}\text{I}$ -BH-CCK-9 was separated from free radioligand by washing twice with PBS containing 2 % BSA. Cell associated  $^{125}\text{I}$ -BH-CCK-9 was recovered by adding 0.5 ml of 0.1 N NaOH to each well and counting the radioactivity in a gamma counter. Nonspecific binding (determined in presence of 1 $\mu\text{M}$  CCK) was always less than 10 % of the total binding. Binding assays were performed in duplicate in at least three separate experiments. Binding data were determined using the nonlinear, least squares, curve fitting computer program, Ligand (Munson and Rodbard, 1980), and GraphPad Prism Program (Software).

Measurement of total inositol phosphates (IP) accumulation - Twenty four hours after COS-7 cell transfection, the transfected cells were transferred to 24-wells culture plates and incubated overnight in DMEM with 2  $\mu\text{Ci}$  /well of myo-2- $^3\text{H}$ inositol (18.6 Ci/mmol) (Amersham). Following the aspiration of the medium containing the  $^3\text{H}$  myo-inositol, the cells were incubated at 37 °C for 20 min with 1 ml of DMEM containing 20 mM LiCl. The cells were then washed with IP buffer pH 7.45 (20 mM Hepes, 135 mM NaCl, 2 mM  $\text{CaCl}_2$ , 1.2 mM  $\text{MgSO}_4$ , 1 mM EGTA, 10 mM LiCl, 11.1 mM glucose and 0.5% BSA) and then incubated one hour at 37° C with IP buffer containing the indicated concentrations of peptide. The reaction was stopped by adding 1 ml of methanol/HCl to each well and the contents transferred to an AG 1-X8 column (formate form) (Bio-Rad, France). Each column was washed twice with 3 ml water followed by 2 ml of 5 mM sodium tetraborate/60 mM sodium

formate. Total inositol phosphates (IP) were eluted from the columns with 2 ml of 1 M ammonium formate/100mM formic acid. [<sup>3</sup>H]myo-inositol phosphate radioactivity was counted in a liquid scintillation counter (Packard, Downers Grove, IL). The EC<sub>50</sub> were calculated using GraphPad Prism Program Software.

Locus numbering scheme – The positions of amino acids in the CCK2R are identified by their original numbering and by a consensus numbering (indicated in parentheses) as described previously to facilitate the comparison between different GPCRs (Ballesteros, 1995). Briefly in the consensus numbering, transmembrane amino acids are identified by a transmembrane number followed by the position relative to the most conserved residue in that helix, which is assigned the number 50.

Molecular modeling – The WT-CCK2R and CCK-occupied WT-CCK2R molecular models were built as previously described in (Gales et al., 2003a). Briefly, to dock CCK into this CCK2R model, we took into account our previous mutagenesis data and imposed as constraint the direct contact point identified between the lateral side chains of His207 located in the second extracellular loop and Asp<sup>8</sup> of CCK. While keeping this constraint, the resulting complex was submitted to energy minimization using 250 steps of the steepest descent followed by a conjugated gradient until the r.m.s. gradient was less than 0.001 kcal/mol/Å. A distant dependent dielectric term ( $\epsilon = r$ ) and a 20 Å non-bonded cut-off distance were chosen while the hydrogen bond involved in alpha helices conformation was preserved by applying a generic distance constraint between the backbone oxygen atoms of residue *i* and the backbone nitrogen atoms of residue *i* + 4, excluding prolines. This was performed using the Discover calculation engine with the CVFF force field (InsightII version 2000.1, Accelrys). The minimized coordinates of the wild type and mutated receptor that were constructed using the

**MOL #29967**

Biopolymer module were then used as the starting point for a 150 ps at 300 K using the Verlet algorithm while the constraint used during minimization was maintained. The resulting conformation was then further minimized using a 250 steps of the steepest descent followed by a conjugated gradient until the r.m.s. gradient was less than 0.001 kcal/mol/Å. The comparison of the structure of mutant receptor with that of the wild type receptor was performed using the Search Compare module. In each transmembrane domain, the C $\alpha$  of the most conserved amino acids were chosen for superposition: Asn72(N1.50), Asp100(N2.50), Arg152(R3.50), Trp179(W4.50), Pro230(5.50), Pro353(6.50), Pro392(7.50).

The program package (Insight II, Discover, Search Compare, Homology, Biopolymer) from Accelrys (San Diego, CA) was used for all the calculations.

## RESULTS

### *Identification of the residues of the CCK2R that interact with Trp<sup>6</sup> of CCK by using molecular modeling.*

We previously reported that the replacement of Trp<sup>6</sup> by Ala in non sulfated CCK-9 induced a dramatic decrease in both the affinity (no binding measurable) and potency (around 13 000-fold) of the modified [Ala<sup>6</sup>]CCK-9 for the WT-CCK2R as well as in its efficacy to stimulate IP production (32 %) (Silvente-Poirot et al., 1999), suggesting that Trp<sup>6</sup> is important for CCK binding and activity. In the present work, we used the CCK-occupied WT-CCK2R molecular model that we have described (Gales et al., 2003a), to identify the amino acids in interaction with Trp<sup>6</sup>. As shown in Fig.1a, the indole group of Trp<sup>6</sup> is positioned into a cavity in the receptor formed by Phe120 (located in the first extracellular loop (ECL1), His381(H7.39) and Tyr385(Y7.43) (located at the top of transmembrane 7 (TM7)) and is delineated by residues Phe110(F2.60) and Ser137(S3.35) (located at the top of TM2 and in TM3 respectively). A network of interactions linked these different residues. A stacking interaction was observed between the phenyl rings of Trp<sup>6</sup> and Phe120 (distance between centroids 7.6 Å) (McGaughey et al., 1998), while the pyrrole part of Trp<sup>6</sup> formed a T-shape interaction with both the phenyl ring of Tyr385(Y7.43) and the imidazole of His381(H7.39) (distance 4.8 Å and 4.0 Å) (McGaughey et al., 1998). A van der Waals interaction was observed between the phenolic ring of Tyr385(Y7.43) and the imidazole group of His381(H7.39) with a distance of 3.8 Å. Moreover, the oxygen of the hydroxyl group of S137(S3.35) located at the vicinity of Trp<sup>6</sup> was hydrogen bonded with the hydroxyl group of Tyr385(Y7.43) (distance 1.8 Å) while the side chain of Phe110(F2.60) was involved in a van der Waals interaction with the indole group of Trp<sup>6</sup> (distance 3.1 Å).

*Effects of exchanging Trp<sup>6</sup> of sulfated CCK-9 on binding and biological activity for the WT-CCK2R.*

Since the effect of exchanging Trp<sup>6</sup> for Ala was previously evaluated on non-sulfated CCK-9 peptides, we first tested the same exchange on sulfated CCK-9s to evaluate the exact contribution of this residue to the affinity and activity to stimulate IP production in COS cells expressing the WT-CCK2R, and then tested other modifications at this position based on the interactions identified in the molecular model. As shown in table 1, the exchange of Trp<sup>6</sup> for Ala induced an important effect on the affinity and activity of sulfated [Ala<sup>6</sup>]-CCK-9s peptide for the WT-CCK2R since a decrease of 4 400- and 2 467-fold in the affinity and potency were measured, while the efficacy to produce IP was decreased by about 36 %. Interestingly, the exchange of Trp<sup>6</sup> by Phe, an other aromatic residue in the [Phe<sup>6</sup>]-CCK-9s peptide, had an effect close to that of the Ala exchange, by decreasing 1 126- and 831-fold the affinity and potency of the modified peptide and by 15 % its efficacy. The important effect measured while the aromatic property of the residue was conserved is consistent with the interaction of Trp<sup>6</sup> with several residues of the receptor as indicated in the molecular model. We then tested the exchange of Trp<sup>6</sup> for Ala- $\alpha$ -Naphthyl to keep two aromatic phenyl rings. This exchange induced a much smaller effect than the two previous modifications since the affinity and potency of the modified [Ala<sup>6</sup>- $\alpha$ -Naphthyl]-CCK-9s peptide was decreased by 41- and 43-fold with no change on its efficacy to produce IP. Together these data are consistent with the molecular model that shows Trp<sup>6</sup> in interaction with a cluster of residues via the phenyl and pyrrole parts of its indole group (Fig.1a).

*Effects of the Phe120 Trp mutation on binding and biological activity of the CCK2R.*

In agreement with the involvement of Phe120 in the CCK binding site, we have reported, in a previous study, that the mutation of Phe120 to Ala resulted in an important decrease in CCK binding and potency to stimulate inositol phosphates (IP) production (no detectable binding of labeled CCK and a 440-fold decrease in the EC<sub>50</sub>, but normal expression and binding of the antagonist [<sup>3</sup>H] PD140376) (Silvente-Poirot et al., 1998). To characterize further the interaction of Phe120 with Trp<sup>6</sup>, we mutated Phe120 to Trp and investigated the consequences of this mutation on CCK binding and activity after transient transfection of the mutant and wild type receptors into COS cells. We hypothesized that the interaction of a Trp pair should not or slightly modify the affinity of CCK for the Trp120 mutant compared to the F120A mutation that removed the aromatic group of the residue. As reported in table 2, the F120W mutation induced a gain of affinity and function since a 5-fold increased affinity and potency of CCK for the F120W mutant and full efficacy (E<sub>max</sub>) was measured compared with the WT-CCK2R. Interestingly, a 2.3-fold increase in basal IP production was detected compared with the control cells. We then evaluated the effects of exchanging Phe120 to Trp in the molecular model. The only difference that was observed in the binding site between the CCK-occupied F120W model and the CCK-occupied WT-CCK2R model was that the distance between the aromatic side chains of Trp<sup>6</sup> of CCK and Trp120 was decreased by about 1 Å compared with that measured between Phe120 and Trp<sup>6</sup> of CCK in the CCK-occupied WT-CCK2R model (Fig.1b). Consequently, this decrease distance resulted to strengthen the interactions between Trp120 and Trp<sup>6</sup> as well as with the other amino acids surrounding Trp<sup>6</sup> as indicated by the representation of the van der Waals volumes (Fig.1c and Fig.1d). Together, these data are consistent with an interaction between Phe120 and Trp<sup>6</sup> of CCK.

*Characterization of the constitutive activity of mutations at position 120 in the CCK2R.*

Since we measured an increase in the basal IP production for the F120W mutant, we determined whether this increase was dependent on the F120W mutant expression and whether this effect was specific or not of this mutation by testing different substitutions at this position. The increase in basal IP production was shown to be correlated with increased level of the F120W mutant expression while no change was observed for the WT-CCK2R when its expression was increased (Fig.2a). In addition, the basal activity was reversed by RPR048, the inverse agonist that we have previously characterized as a blocker of the constitutive activity of an other mutant (E151A) of the CCK2R (Gales et al., 2003b) (Fig.2b). These data show that the F120W mutant harboured constitutive activity on IP production. We then mutated Phe120 to aromatic (Tyr), polar (His) or aliphatic (Met and Leu) residues and evaluated the effects of these mutations on CCK binding as well as on basal and CCK-stimulated IP production.

As shown in table 2, the mutation of Phe120 to Tyr, that conserved the aromatic phenyl group, had a small effect on CCK affinity and potency to stimulate IP (19- and 16-fold decrease respectively) while the mutation of Phe120 to residues His, Met and Leu had a more important effects by decreasing the affinity of CCK by 139, 215 and 275-fold respectively and its potency to stimulate IP production by 86-, 142- and 201-fold respectively. For all these mutants, no increase in basal IP production was measured compared to the control cells (table 2). Similarly, no constitutive IP production was measured with the F120A mutation previously described (table 2). Together these data suggest that the constitutive activity of the F120W mutant is specific of the Trp residue introduced at position 120.

*Effects of the His381(H7.39), Tyr385(Y7.43), Phe110(F2.60) and Ser137(S3.35) mutations on CCK binding and receptor activation.*

We then mutated the other residues (His381(H7.39), Tyr385(Y7.43), Phe110(F2.60) and Ser137(S3.35)) shown to surround Trp<sup>6</sup> in the CCK-occupied WT-CCK2R molecular model, to determine their contribution to CCK binding and receptor activity. These different residues were mutated to Ala to evaluate the contribution of their side chains after their transfection into COS cells. As reported in Table 3, the analysis of the maximal binding capacities (B<sub>max</sub>) demonstrated that all these mutants displayed a similar level of cell surface expression compared with the WT-CCK2R. The analysis of CCK competition binding revealed that only the H381A(H7.39A) and Y385A(Y7.43A) mutations resulted in a significant decrease in CCK affinity (83- and 89-fold respectively) compared with the WT-CCK2R. The decrease in CCK affinity observed for the H381A and the Y385A mutants is in accordance with the molecular model. The phenyl ring of Phe110(F2.60) does not seem to have an important contribution on CCK binding since no change in CCK affinity was observed after its removal. The slight effect (1.7-fold) observed on CCK affinity for the S137A mutant indicates that Ser137(S3.35) is also not essential for CCK affinity, and is in agreement with the molecular model that predicts a preferential hydrogen bond interaction with the hydroxyl group of Tyr385(Y7.43).

We then determined the importance of His381(Y7.39), Tyr385(Y7.43), Phe110 (F2.60) and Ser137(S3.35) residues in the activation of the CCK2R by testing the capacity of the corresponding Ala mutants to induce basal and CCK-stimulated IP production. None of these mutants displayed increased basal activity compared with the control cells (Table 3). The potency of CCK for the H381A and Y385A mutants was decreased 56- and 59-fold compared with the WT-CCK2R while no change were measured with the F110A and S137A

mutants. Thus, there is a good correlation between the potency and affinity of CCK for these different mutants. In contrast, all the mutants displayed a decreased efficacy to stimulate IP production (32 % for the F110A mutant and around 50 % for the H381A, Y385A and S137A mutants), indicating that all these residues participate in the receptor activation while only His381(Y7.39) and Tyr385(Y7.43) are involved in CCK binding and activity. These data are consistent with an involvement of these residues in a signaling cascade initiated by Trp<sup>6</sup>.

*Molecular modeling of the constitutively active F120W mutant.*

The fact that the mutation of Phe120 to other residues (Ala, Leu, His, Met, Tyr) than Trp did not confer constitutive activity to the receptor but in contrast significantly decreased CCK binding and activity, suggested that Phe120 is not involved in an intramolecular bond that stabilized the receptor in its inactive state as described for most constitutively active mutants described so far (Cotecchia et al., 2003; Parnot et al., 2002). To study further the contribution of this residue in the activation of the CCK2R as well as in the inactive state of the CCK2R, we built a molecular model of the F120W-CCK2R mutant (“constitutively active F120W model”). This model was then compared with the CCK-occupied WT-CCK2R (“active model”) and the non-occupied WT-CCK2R (“inactive model”) molecular models. As shown in Fig. 3, when we compared the “active” (Fig. 3a) and the “inactive” (Fig. 3b) models, it appeared that in the “inactive model” the aromatic ring of Phe120 formed a stacking interaction with that of Phe110(F2.60). Similarly, the phenyl group of Tyr385(Y7.43) stacked with the imidazole ring of His381(H7.39). In the “active model”, the insertion of CCK and the interaction of the indole group of Trp<sup>6</sup> with the phenyl ring of Phe120 resulted in the breaking of this stacking and the release of the phenyl group of Phe110(F2.60) that turned down. In addition, the imidazole group of His381(H7.39) and the phenyl group of

Tyr385(Y7.43) turned over to interact with the indole group of Trp<sup>6</sup>. This movement preserved the interaction between the lateral chains of His381(H7.39) and Tyr385(Y7.43). Interestingly, in the “constitutively active F120W model”, similar changes occurred when Phe120 was replaced by Trp120 since the side chains of Phe110(F2.60), His381(H7.39) and Tyr385(Y7.43) moved as in the “active model” (Fig. 3c), while no significant movements were observed for His207 (ECL2) and Asn358(N6.55)/Tyr189(Y4.60) that interact with Asp<sup>8</sup> and Phe<sup>9</sup>-NH<sub>2</sub> of CCK respectively (Silvente-Poirot et al J Biol Chem 1999; Gales et al, Mol Pharmacol. 2003a) (not illustrated). These results suggest that the introduction of a Trp at position 120 mimics the effects of Trp<sup>6</sup> of CCK and may explain the constitutive activity of this mutation compared to the others mutations tested.

#### *Conformational changes involved during the CCK2R activation*

Since the experimental data were found to be in accordance with the theoretical models that we built we analysed further the conformational changes that occurred in transmembranes and intracellular loops of the “inactive” and “active” models in comparison with the “constitutively active F120W” model. When we compared the “inactive model” (Fig. 4a) with the “active model” (Fig. 4b), we observed that the binding of CCK induced a descent of TM2 and TM3 of 3.6 Å toward the cytosol while TM4 underwent a significant lateral shift of 4.7 Å away from TM3, that resulted in the breaking of the hydrogen bond linking Ser131(S3.29) and Thr193(T4.64) (Fig. 4d and 4e).

In the “inactive model” (Fig. 5a), the oxygens of the carboxyl of Glu151(E3.49) of the highly conserved E/DRY motif, located at the end of TM3, established two hydrogen bonds with the hydroxyl of Ser95(S2.45) and the NH of the peptidic bond of Leu94(L2.44), distances of 1.8 Å and 1.4 Å respectively. Moreover, the end of TM4 was connected to the

C-terminal part of the third intracellular loop via a hydrophobic interaction between the aliphatic side chain of Val174(V4.45) and Leu330 (ICL3) respectively (distance 2.4 Å) while the guanido group of Arg158 (ICL2) formed a hydrogen bond with the oxygen of the amide group of Gln327 (ICL3) (distance: 1.9 Å).

In the “active model” (Fig 5b), the motion of TM3 toward the cytosol resulted in the exposure of Glu151(E3.49). The descent of TM2 and TM3 while maintaining the hydrogen bond between the hydroxyl of Ser95(S2.45) and the carboxyl group of Glu151(E3.49), resulted in the breaking of the hydrogen bond with the NH of Leu94(L2.44). These movements and the lateral movement of TM4 in the “active” model induced the disruption of the interaction between the aliphatic sides chains of Val174(V4.45) and Leu330 (ICL3) (distance 9 Å). These transmembrane domains motions were followed by a movement of the second and third intracellular loops away from each other. The movement of these loops resulted in the breaking of the hydrogen bond between the guanido group of Arg158 (ICL2) and the amide group of Gln327 (ICL3), and the subsequent establishment of a hydrogen bond between the NH of the amide group of Gln327 and the carboxyl group of Glu151(E3.49) (distance: 1.8 Å). These changes enabled Glu151(E3.49) to interact with the aliphatic side chains of Leu330 (ICL3) (distance 3.2 Å), Leu94(L2.44) (distance 4.6 Å) and Leu93(L2.43) (distance 3.1 Å) that formed a hydrophobic pocket surrounding its cytoplasmic side, as well as the release and exposure of the guanido side chain of Arg158 in the groove formed in between the second and third intracellular loops.

In the “constitutively active F120W model”, similar movements were observed (Fig. 4c). However, while a similar descent of TM2 and TM3 of 3.6 Å toward the cytosol was measured, the lateral movement of TM4 was less marked (3.3 Å) compared with that in the “active model” (4.7 Å), however this motion resulted in the disruption of the interaction

between Ser131 and Thr193 (Fig. 4f). These movements induced the exposure of Glu151(E3.49), however the interaction of Glu151(E3.49) differed from that observed in the “active model” since the oxygens of its carboxyl group were involved in a hydrogen bond with a NH<sub>2</sub> of the guanido group of the adjacent Arg152(R3.50) (distance 1.6 Å) and with the hydroxyl of Ser95(S2.45) (distance 1.4 Å); while Gln327 (ICL3) was too far away to be involved in such a bond (distance 8.2 Å). However, as in the “active model”, these conformational changes meant that Glu151(E3.49) interacted with hydrophobic residues Leu330 (ICL3) (distance 4.3 Å), Leu94(L2.44) (distance 4.6 Å), Leu93(L2.43) (distance 2.6 Å) after the disruption of the interaction between Leu330 and Val174(V4.45) (distance 8.2 Å). Finally, as observed in the “active model”, these movements ended up in the release and exposure of Arg158.

Thus, the “active” and “constitutively active F120W” models indicate that part of the activation of the CCK2R results in the exposure and protonation of Glu151(E3.49) as well as in the formation of an amphiphatic pocket surrounding Glu151(E3.49) and involving Leu330, and in the exposure and release of Arg158 located in the ICL2.

*Effect of mutating Glu151(E3.49), Leu330, Arg158, Ser131(S3.29) and Thr193(T4.64) on the CCK2R activation.*

We have reported previously that the mutation of the Glu151(E3.49) to Ala in the human CCK2R induced constitutive activation of IP production and conferred transforming as well as tumorigenic properties on the corresponding E151A mutant, indicating that Glu151(E3.49) is a key residue for the CCK2R activation. In addition, the mutation of Leu325 to Glu in the human CCK2R (the corresponding residue of Leu330 in the rat CCK2R) has been reported to constitutively activate IP production (Beinborn et al., 1998). Therefore, we

**MOL #29967**

have performed similar mutations in the rat CCK2R to determine whether these two mutants were constitutively active. Indeed, the E151A and L330E mutants constitutively activated IP production to the same extent as the F120W mutant compared to the control cells (Table 3).

We then mutated Arg158, Ser131(S3.29) and Thr193(T4.64) to Ala to determine the effects of these mutations on binding and IP production. As reported in Table 3, these mutations did not affect the binding capacity nor the affinity and potency of CCK. In contrast, the efficacy was decreased by 30 % for the R158A mutant and 46 % for the S131A and T193A mutants, indicating that these residues are involved in the CCK2R activation, consistent with that observed in the “active” molecular model.

## DISCUSSION

The present work was undertaken to identify the residues in the CCK2R that interact with Trp<sup>6</sup> of CCK for which no receptor partners had yet been identified and to gain insight into the mechanisms of peptide-induced activation by combining mutagenesis, pharmacology and molecular modelling studies. Molecular modelling of GPCRs presents different limitations due to, the fact that only one high resolution crystal structure of a GPCR is available (rhodopsin), the lack of well defined secondary structure for the intracellular loops that are flexible as well as the approximations of MD stimulations (Fanelli F et al, 2005). Despite these limitations, the modelling analysis performed in the present study within the same approximations, has been able, in combination with experimental data, to complete the mapping of CCK binding site and to infer a few structural features that differentiate the inactive from the active and constitutively active receptor states. The molecular model of the CCK-occupied CCK2R, that we previously validated, was used to identify the residues in interaction with Trp<sup>6</sup> of CCK. A cluster of residues surrounding Trp<sup>6</sup> were identified as putative partners both in TM domains (His381, Tyr385, Ser137, Phe110) and in the first extracellular loop (Phe120). Previous and present experimental data confirmed the molecular model predictions. Indeed, we previously reported the importance of Phe120 for CCK affinity and activity after its mutation to Ala (Silvente-Poirot et al., 1998). In the present study, further support for an interaction of Trp<sup>6</sup> with Phe120 was obtained by mutating Phe120 to Trp. The F120W mutant bound CCK with a 5-fold increased affinity and potency compared with the WT-CCK2R, and displayed constitutive activity. This gain of affinity and activity, that contrasted with the significant decrease in affinity and potency measured for the F120A, F120Y, F120L, F120H and F120M mutants, indicated that the mutation of Phe120 to Trp

favoured a better interaction with Trp<sup>6</sup> and is consistent with an interaction between Phe120 and Trp<sup>6</sup>. In accordance with the experimentation, the exchange of Phe120 to Trp in the CCK2R-CCK molecular model strengthened the interaction between the indole groups of Trp<sup>6</sup> and Trp120 by reducing their distance to about 1 Å.

The involvement of His381(H7.39) and Tyr385(H7.43) in CCK binding and activity were shown by exchanging these residues to Ala. Their mutations resulted in a significant decrease in CCK affinity and potency (80-fold) as well as efficacy (50 %). The similar decrease in CCK affinity measured for these two mutants is consistent with the molecular model that predicted a stacking interaction between these residues. The mutation of Ser137(S3.35) and Phe110(F2.60) to Ala were shown to be important for the receptor activity since their mutations only decreased their efficacies to produce IP by 50 and 30 % respectively. It has to be noted that the decrease in CCK efficacy for these different mutants is in the same range than the decrease in efficacy measured for the sulfated [Ala<sup>6</sup>]CCK-9s peptide toward the WT-CCK2R (36 %), consistent with an involvement of these residues in a signaling cascade initiated by Trp<sup>6</sup>.

Since Trp<sup>6</sup> is involved in a complex network of interactions, it is difficult to assess the energetic contribution of a single interaction. The simultaneous presence of multiple interactions produces cooperativity between them, and together they can be much stronger than might be expected from the sum of their individual strengths (Creighton, 1993). The important decrease in CCK affinities measured when Phe120, His381(H7.39) and Tyr385(7.43) are mutated to Ala (respectively 440-, 83, 73-fold) is consistent with the complex network of interactions linking Trp<sup>6</sup> with these residues.

Identification and studies using constitutively active mutants have helped the understanding of receptor activation by showing that, in absence of agonist, receptors are kept

inactive by constraining intramolecular interactions. The constitutively active mutations described so far were shown to release such constraints leading to receptor activation (Cotecchia et al., 2003; Parnot et al., 2002). In the present study, experimental and modeling data provide original data on the activation processes of the CCK2R initiated by Trp<sup>6</sup>. Indeed, the mutation of Phe120 to Trp was shown to cause constitutive PLC activation, however our data indicate that Phe120 is not involved in an intramolecular bond that maintains the receptor in an inactive state. Firstly, its mutation to different residues Ala, Leu, Tyr, His, and Met did not confer constitutive activity to the CCK2R as would be expected when a constraint is removed, suggesting that the constitutive activity of the F120W mutant is specific of the Trp residue introduced at position 120. Conversely, the mutation of Phe110(F2.60) to Ala, that removed the interactions between the aromatic rings of Phe120 and Phe110(F2.60) in the molecular model, did not induce constitutive activation of the receptor. Moreover, the construction of a molecular model of the constitutively active F120W mutant highlights that the introduction of a Trp at position 120 mimics the effects of Trp<sup>6</sup> of CCK on receptor activation since similar movements of Phe110(F2.60), Tyr385(Y7.43) and His381(H7.39) were observed in the “active model” after the interaction of Trp<sup>6</sup> of CCK with Phe120, His381(H7.39) and Tyr385(Y7.43), and in the “constitutively active F120W model” when Phe120 was exchanged by Trp.

Thus, both in the “active” and the “constitutively active F120W” models, CCK binding induces a movement of TM2 and TM3 of 3.6 Å toward the cytosol while a significant translation of TM4 occurs away from TM3. These movements of the transmembrane domains result in: i) the exposure of Glu151(E3.49) of the highly conserved E/DRY motif (TM3) ii) the disruption of the interaction between Val174 (V4.45) and Leu330 (ICL3) and the

formation of an amphiphatic pocket involving protonated Glu151(E3.49) and Leu330 iii) the opening of the intracellular loops 2 and 3 that results to the exposure of Arg158.

Some differences were also observed between these models. In the “active” model, the side chain of Glu151(E3.49) interacts with that of Gln327 via a hydrogen bond, while in the “constitutively active F120W” model, it forms a hydrogen bond with the side chain of Arg152(R3.50) and not with that of Gln327 that is too far away to be involved in such a bond (distance 8.3 Å). These differences between these two models could be due to the weaker movement of TM4 in the “constitutively active F120W” model (3.3 Å) compared with that measured in the “active model” (4.7 Å) that does not enable Gln327 to interact with Glu151(E3.49). More likely, in the “active model”, the interaction of the C-terminal amidated Phe<sup>9</sup> of CCK with Tyr189(Y4.60) located in TM4 amplifies the translational movement of TM4 (Gales et al., 2003a). Thus, a significant motion of TM4 seems to contribute to the maximal activation of PLC by CCK, in addition to other domains like ECL2, TM6 and TM7 which involved important residues for CCK binding and Gq activation (Blaker et al., 1998; Silvente-Poirot et al, 1999; Gales et al., 2000; Gales et al., 2003a). Cross-linking studies of rhodopsin with a photoactivated chromophore have shown a flip-over of the ionone ring of retinal from TM6 to TM4 during receptor activation implying that movements of TM3 and TM4 accompany receptor activation (Borhan et al., 2000).

Glu151(E3.49) appears as an other key element in the CCK2R activation. Its mutation to Ala confers constitutive activity to the corresponding E151A mutant both in human CCK2R (Gales et al., 2003b) and in the rat CCK2R (present study). The charge neutralizing mutation of this Asp/Glu residue has been reported to induce constitutive activation of a number of GPCRs (Alewijnse et al., 2000; Ballesteros et al., 2001; Cohen et al., 1993; Rasmussen et al., 1999; Scheer et al., 1997). Direct evidence for protonation of this residue in

rhodopsin by the uptake of a proton during photoactivation has been reported (Arnis et al., 1994). In the crystal structure of the inactive state of rhodopsin, Glu134(E3.49) is connected to the next Arg135(R3.50), while Arg135(R3.50) is in interaction with Glu247(E6.30) and Thr251(T6.34) located in TM6. Similar interactions have been demonstrated in the  $\beta$ 2-adrenergic receptor (Ballesteros et al., 2001). However, Glu247(E6-30) is not conserved among all the rhodopsin-like receptors indicating that other interactions might serve the same function in receptors lacking this residue. In the WT-CCK2R, Glu247(E6.30) is not conserved, and no acidic residue is present at the end of TM6 to establish an interaction with Arg135(R3.50). Only, the C-terminal part of the third intracellular loop is connected to TM4 via the interaction of Leu330 with Val174(V4.45). Interestingly, the mutation of this Leu to Glu in the human and rat CCK2R induced constitutive activation (Beinborn et al., 1998) and present study. Consistent with a role of Leu330 in the activation of the CCK2R, the “active” and “constitutively active F120W” models reveal that Leu330 is involved in the disruption of the bond linking Arg158 and Gln327 by participating in the formation of the amphiphatic pocket involving Glu151(E3.49). In agreement with a role for Arg158 in the CCK2R activation, its mutation to Ala decreased maximal IP response by 30 % without affecting CCK binding and potency. This decrease in efficacy is in the same range than that measured when Trp<sup>6</sup> was exchanged to Ala in CCK, suggesting that Arg158 participates in the activation cascade initiated by Trp<sup>6</sup> of CCK.

In conclusion, the present study enabled us to complete the mapping of CCK binding site and to explore receptor conformational changes initiated by the ligand and during constitutive activation. Understanding these different processes will help in the design of inverse agonists to inhibit the constitutive activation of the CCK2R. Importantly, constitutive

MOL #29967

activation of the CCK2R may have a pathological relevance since a variant that displays constitutive cell proliferation and PLC activation has been isolated in different human cancers (Ding et al., 2002; Harris et al., 2004; Hellmich et al., 2000) and we have reported that the constitutively active E151A mutant is highly tumorigenic when expressed in NIH-3T3 cells (Gales et al., 2003b).

## **Footnotes**

<sup>1</sup> MRP and CD: both authors equally contributed to the work.

<sup>2</sup> SSP: is in charge of research for the CNRS.

This work was supported by the INSERM, AFFICHEM, Institut Claudius Regaud and French Ministry of Education and Research.

Reprint request to corresponding author:

Dr Sandrine Silvente-Poirot,

INSERM U563, Equipe : Métabolisme, Oncogénèse et différenciation cellulaire,

Institut Claudius Regaud

20-24 rue du Pont Saint Pierre, 31052 Toulouse Cedex, France

Tel : 33 5 61 42 46 48 ; Fax : 33 5 61 42 46 31

Email : [poirot.sandrine@claudiusregaud.fr](mailto:poirot.sandrine@claudiusregaud.fr)

## REFERENCES

- Alewijnse AE, Timmerman H, Jacobs EH, Smit MJ, Roovers E, Cotecchia S and Leurs R (2000) The effect of mutations in the DRY motif on the constitutive activity and structural instability of the histamine H<sub>2</sub> receptor. *Mol Pharmacol* **57**:890-898.
- Aly A, Shulkes A and Baldwin GS (2004) Gastrins, cholecystokinins and gastrointestinal cancer. *Biochim Biophys Acta* **1704**:1-10.
- Arnis S, Fahmy K, Hofmann KP and Sakmar TP (1994) A conserved carboxylic acid group mediates light-dependent proton uptake and signaling by rhodopsin. *J Biol Chem* **269**:23879-23881.
- Ballesteros JA, Jensen AD, Liapakis G, Rasmussen SG, Shi L, Gether U and Javitch JA (2001) Activation of the beta 2-adrenergic receptor involves disruption of an ionic lock between the cytoplasmic ends of transmembrane segments 3 and 6. *J Biol Chem* **276**:29171-29177.
- Ballesteros J. A. and Weinstein H (1995) Integrated methods for the construction of three dimensional models and computational probing of structure-function relations in G protein-coupled receptors. *Methods Neurosci* **25**:366-428.
- Beinborn M, Quinn SM and Kopin AS (1998) Minor modifications of a cholecystokinin-B/gastrin receptor non-peptide antagonist confer a broad spectrum of functional properties. *J Biol Chem* **273**:14146-14151.
- Blaker M, Ren Y, Gordon MC, Hsu JE, Beinborn M and Kopin AS (1998) Mutations within the cholecystokinin-B/gastrin receptor ligand 'pocket' interconvert the functions of nonpeptide agonists and antagonists. *Mol Pharmacol* **54**:857-863.
- Borhan B, Souto ML, Imai H, Shichida Y and Nakanishi K (2000) Movement of retinal along the visual transduction path. *Science* **288**:2209-2212.
- Cohen GB, Yang T, Robinson PR and Oprian DD (1993) Constitutive activation of opsin: influence of charge at position 134 and size at position 296. *Biochemistry* **32**:6111-6115.
- Cotecchia S, Fanelli F and Costa T (2003) Constitutively active G protein-coupled receptor mutants: implications on receptor function and drug action. *Assay Drug Dev Technol* **1**:311-316.
- Creighton TE (1993) *Protein, structure and molecular properties*. W.H. Freeman and Company, New York.
- de Tullio P, Delarge J and Pirotte B (2000) Therapeutic and chemical developments of cholecystokinin receptor ligands. *Expert Opin Investig Drugs* **9**:129-146.
- Ding WQ, Kuntz SM and Miller LJ (2002) A misspliced form of the cholecystokinin-B/gastrin receptor in pancreatic carcinoma: role of reduced cellular U2AF35 and a suboptimal 3'-splicing site leading to retention of the fourth intron. *Cancer Res* **62**:947-952.
- Doi T, Molday RS and Khorana HG (1990) Role of the intradiscal domain in rhodopsin assembly and function. *Proc Natl Acad Sci U S A* **87**:4991-4995.
- Fanelli F and De Benedetti P.G (2005) Computational modeling approaches to structure-function analysis of G protein-coupled receptors. *Chem Rev* **105**: 3297-3351.
- Gales C, Kowalski-Chauvel A, Dufour MN, Seva C, Moroder L, Pradayrol L, Vaysse N, Fourmy D and Silvente-Poirot S (2000) Mutation of Asn-391 within the conserved

- NPXXY motif of the cholecystokinin B receptor abolishes Gq protein activation without affecting its association with the receptor. *J Biol Chem* **275**:17321-17327.
- Gales C, Poirot M, Taillefer J, Maigret B, Martinez J, Moroder L, Escrieut C, Pradayrol L, Fourmy D and Silvente-Poirot S (2003a) Identification of tyrosine 189 and asparagine 358 of the cholecystokinin 2 receptor in direct interaction with the crucial C-terminal amide of cholecystokinin by molecular modeling, site-directed mutagenesis, and structure/affinity studies. *Mol Pharmacol* **63**:973-982.
- Gales C, Sanchez D, Poirot M, Pyronnet S, Buscail L, Cussac D, Pradayrol L, Fourmy D and Silvente-Poirot S (2003b) High tumorigenic potential of a constitutively active mutant of the cholecystokinin 2 receptor. *Oncogene* **22**:6081-6089.
- Gether U (2000) Uncovering molecular mechanisms involved in activation of G protein-coupled receptors. *Endocr Rev* **21**:90-113.
- Harris JC, Clarke PA, Awan A, Jankowski J and Watson SA (2004) An antiapoptotic role for gastrin and the gastrin/CCK-2 receptor in Barrett's esophagus. *Cancer Res* **64**:1915-1919.
- Hellmich MR, Rui XL, Hellmich HL, Fleming RY, Evers BM and Townsend CM, Jr. (2000) Human colorectal cancers express a constitutively active cholecystokinin-B/gastrin receptor that stimulates cell growth. *J Biol Chem* **275**:32122-32128.
- Javitch JA, Shi L, Simpson MM, Chen J, Chiappa V, Visiers I, Weinstein H and Ballesteros JA (2000) The fourth transmembrane segment of the dopamine D2 receptor: accessibility in the binding-site crevice and position in the transmembrane bundle. *Biochemistry* **39**:12190-12199.
- McGaughy GB, Gagne M and Rappe AK (1998) pi-Stacking interactions. Alive and well in proteins. *J Biol Chem* **273**:15458-15463.
- Munson PJ and Rodbard D (1980) Ligand: a versatile computerized approach for characterization of ligand-binding systems. *Anal Biochem* **107**:220-239.
- Parnot C, Miserey-Lenkei S, Bardin S, Corvol P and Clauser E (2002) Lessons from constitutively active mutants of G protein-coupled receptors. *Trends Endocrinol Metab* **13**:336-343.
- Rasmussen SG, Jensen AD, Liapakis G, Ghanouni P, Javitch JA and Gether U (1999) Mutation of a highly conserved aspartic acid in the beta2 adrenergic receptor: constitutive activation, structural instability, and conformational rearrangement of transmembrane segment 6. *Mol Pharmacol* **56**:175-184.
- Ren Y, Blaker M, Seshadri L, McBride EW, Beinborn M and Kopin AS (2003) Conserved cholecystokinin receptor transmembrane domain IV amino acids confer peptide affinity. *J Mol Neurosci* **20**:115-124.
- Reubi JC, Schaer JC and Waser B (1997) Cholecystokinin(CCK)-A and CCK-B/gastrin receptors in human tumors. *Cancer Res* **57**:1377-1386.
- Rozengurt E and Walsh JH (2001) Gastrin, CCK, signaling, and cancer. *Annu Rev Physiol* **63**:49-76.
- Scheer A, Fanelli F, Costa T, De Benedetti PG and Cotecchia S (1997) The activation process of the alpha1B-adrenergic receptor: potential role of protonation and hydrophobicity of a highly conserved aspartate. *Proc Natl Acad Sci U S A* **94**:808-813.
- Schwartz TW, Frimurer TM, Holst B, Rosenkilde MM and Elling CE (2006) Molecular mechanism of 7TM receptor activation--a global toggle switch model. *Annu Rev Pharmacol Toxicol* **46**:481-519.

MOL #29967

- Shi L and Javitch JA (2002) The binding site of aminergic G protein-coupled receptors: the transmembrane segments and second extracellular loop. *Annu Rev Pharmacol Toxicol* **42**:437-467.
- Shi L and Javitch JA (2004) The second extracellular loop of the dopamine D2 receptor lines the binding-site crevice. *Proc Natl Acad Sci U S A* **101**:440-445.
- Silvente-Poirot S, Escrieut C, Gales C, Fehrentz JA, Escherich A, Wank SA, Martinez J, Moroder L, Maigret B, Bouisson M, Vaysse N and Fourmy D (1999) Evidence for a direct interaction between the penultimate aspartic acid of cholecystokinin and histidine 207, located in the second extracellular loop of the cholecystokinin B receptor. *J Biol Chem* **274**:23191-23197.
- Silvente-Poirot S, Escrieut C and Wank SA (1998) Role of the extracellular domains of the cholecystokinin receptor in agonist binding. *Mol Pharmacol* **54**:364-371.
- Silvente-Poirot S and Wank SA (1996) A segment of five amino acids in the second extracellular loop of the cholecystokinin-B receptor is essential for selectivity of the peptide agonist gastrin. *J Biol Chem* **271**:14698-14706.
- Wank SA (1995) Cholecystokinin receptors. *Am J Physiol* **269**:G628-G646.

## LEGENDS FOR FIGURES

**Fig. 1:** Detailed view of the amino acids side-chains in interaction with Trp<sup>6</sup> of CCK in the CCK-occupied WT-CCK2R model (a) and in the CCK-occupied F120W mutant model (b). Oxygen atoms are in red, hydrogen atoms are in white, carbon atoms are in green and nitrogen atoms are in dark blue. Distances (in Å) between chemical functions are represented by dotted lines. Representation of the van der Waals volumes of the amino acids in interaction with or in the vicinity of Trp<sup>6</sup> of CCK in the CCK-occupied WT-CCK2R (c) and CCK-occupied F120W mutant molecular model (d). Phe120 is located in the first extracellular loop (ECL1). According to the Ballesteros and Weinstein nomenclature (Ballesteros, 1995), His381 is H7.39, Tyr385 is Y7.43, Phe110 is F2.60, Ser137 is S3.35.

**Fig. 2 :** **a)** Effect of expression levels of the WT-CCK2R and F120W mutant on the basal level of total IP production. COS cells were transfected with increasing amounts of cDNAs encoding the WT-CCK2R (■) or the F120W mutant (▲). The receptor density (Bmax) and total IP production were measured as described in “Materials and Methods”. **b)** Effect of the inverse agonist RPR038 on basal IP production. COS cells expressing the WT-CCK2R (■) or the F120W mutant (▲) were treated for 1 hour with increasing concentrations of RPR038 and basal IP production was assessed. Results are expressed as increased induction (fold-increase) over control (cells transfected with the empty vector) and are means ± SE of three separate experiments performed in duplicate.

**Fig. 3 :** Comparison of the positioning of His381(H7.39), Tyr385(Y7.43), Phe110(F2.60) and Ser137(S3.35) residues in the three-dimensional models of **a)** the CCK-occupied WT-CCK2R (“active model”); **b)** the non-occupied WT-CCK2R (“inactive model”) and **c)** the F120W mutant (“constitutively active F120W model”). For clarity, only helices (TM) 1, 2, 3 and 7 are displayed. Helices are in green in the “active model”, blue in the “inactive model” and purple in the “constitutively active F120W model”. Oxygen atoms are in red, carbon atoms are in green, and nitrogen atoms are in dark blue.

**Fig. 4 :** Conformational changes involved during receptor activation. **A)** Side view of the three-dimensional models of the non-occupied WT-CCK2R (“inactive model”) (**a**); CCK-occupied WT-CCK2R (“active model”) (**b**) and F120W mutant (“constitutively active F120W model”) (**c**). For clarity, only helices (TM) 3, 4, 6, represented by cylinders, and the intracellular loops ICL2, ICL3, represented by thin ribbons, are displayed to observe the movements of TM3 and TM4 and the opening of the groove between the ICL2 and ICL3. **B)** Side view of the three-dimensional model of the non-occupied WT-CCK2R (“inactive model”) (**d**); CCK-occupied WT-CCK2R (“active model”) (**e**) and the F120W mutant (“constitutively active F120W model”) (**f**) showing the disruption of the hydrogen bond involved between the lateral chains of Ser131 and Thr193. For clarity, only helices (TM) 3, 4 represented by ribbons are shown. According to the Ballesteros and Weinstein nomenclature (Ballesteros, 1995), Ser131 is S3.29 and Thr193 is T4.64.

**Fig. 5:** Comparison of the interactions involved in the intracellular domains of the receptor in the molecular model of the non-occupied WT-CCK2R (“inactive model”) (**a**); CCK-occupied WT-CCK2R (“active model”) (**b**) and F120W mutant (“constitutively active F120W model”)

**MOL #29967**

(c). In the “active model” (b) and “constitutively active F120W model” (c), the changes result in i) the exposure of Glu151(E3.49) of the highly conserved E/DRY motif (TM3) ii) the disruption of the interaction between Val174(V4.45) and Leu330 (ICL3) that results in the formation of an amphiphatic pocket involving protonated Glu151(E3.49) and Leu330 iii) the opening of the intracellular loops (ICL) 2 and 3 which results in the release and exposure of Arg158 (ICL2).

**Table 1 :** Affinities and potencies of CCK modified peptides for the WT-CCK2R transiently expressed in COS cells.  $K_i$  values were calculated from competition curves of  $^{125}\text{I}$ -BH-CCK-9s binding by the indicated peptides. The potencies ( $\text{EC}_{50}$ ) were calculated from the total IP production concentrations-response curves stimulated by the indicated modified peptides. The efficacies ( $\text{E}_{\text{max}}$ ) of the indicated modified peptides to stimulate IP production are expressed as the percent of the maximal increase obtained with 1  $\mu\text{M}$  CCK-9s on cells expressing the WT-CCK2R. The factor  $\text{F}_{\text{CCK-9s}}$  represents the effect of the modified peptide tested on the affinity or potency relative to CCK-9s. Results are expressed as means  $\pm$  SE of three to five separate experiments performed in duplicate.

Ligands	$K_i$ (nM)	$\text{F}_{\text{CCK-9s}}$	$\text{EC}_{50}$ (nM)	$\text{F}_{\text{CCK-9s}}$	$\text{E}_{\text{max}}$ (%)
CCK-9s	$0.72 \pm 0.10$	1	$0.58 \pm 0.14$	1	100
[Ala <sup>6</sup> ]-CCK-9s	$3200 \pm 145$	4400	$1431 \pm 234$	2467	64
[Phe <sup>6</sup> ]-CCK-9s	$811 \pm 59$	1126	$482 \pm 35$	831	85
[Ala- $\alpha$ -Naphthyl <sup>6</sup> ]-CCK-9s	$30 \pm 11$	41	$25 \pm 5$	43	100

**Table 2:** *Pharmacological properties of the WT-CCK2R and F120 mutants transiently expressed in COS cells.* Kd and Bmax values were calculated from the analysis of CCK-9 competition binding using <sup>125</sup>I-BH-CCK-9s as the radioligand. The potencies (EC<sub>50</sub>) of CCK-9 were calculated from the total IP production concentration-response curves. The efficacies (Emax) of CCK-9s to stimulate IP production are expressed as the percent of the maximal increase obtained with 1 μM CCK-9s on cells expressing the WT-CCK2R. The factor Fmut represents the effect of the mutation on CCK-9s affinity or potency relative to the wild type receptor. Basal IP production is expressed as fold increase over that in control cells expressing the empty vector. Results are expressed as means ± SE of three to five separate experiments performed in duplicate. \* Results from (Silvente-Poirot et al., 1998).

Receptor	Kd (nM)	Fmut	Bmax (pmol/10 <sup>6</sup> )	EC <sub>50</sub> (nM)	Fmut	Emax (%)	Basal (x induction)
WT-CCK2R	0.53 ± 0.12	1	1.61 ± 0.14	0.71 ± 0.21	1	100	1.1
F120W mutant	0.10 ± 0.03	0.18	1.59 ± 0.11	0.11 ± 0.05	0.15	100	2.3
F120Y mutant	10.12 ± 1.35	19	1.58 ± 0.35	11.68 ± 2.56	16	100	1.1
F120H mutant	74 ± 15	139	1.59 ± 0.15	61 ± 20	86	100	1.1
F120M mutant	114 ± 12	215	1.62 ± 0.28	101 ± 26	142	100	1.2
F120L mutant	146 ± 23	275	1.45 ± 0.25	143 ± 67	201	93	1.1
F120A mutant*	ND	ND	2.04 ± 1.37	147 ± 38	440	100	1

**Table 3:** *Pharmacological properties of the wild type and mutated CCK2R transiently expressed in COS cells.* Kd and Bmax values were calculated from the analysis of CCK-9s competition binding using <sup>125</sup>I-BH-CCK-9s as the radioligand. The potencies (EC<sub>50</sub>) of CCK-9s were calculated from the total IP production concentrations-response curves. The efficacies (Emax) of CCK-9s to stimulate IP production are expressed as the percent of the maximal increase obtained with 1 μM CCK-9s on cells expressing the WT-CCK2R. The factor Fmut represents the effect of the mutation on CCK-9s affinity or potency relative to the wild type receptor. Basal IP production is expressed as fold increase over that in control cells. Results are expressed as means ± SE of three to five separate experiments performed in duplicate.

Receptor	Kd (nM)	Fmut	Bmax (pmol/10 <sup>6</sup> )	EC <sub>50</sub> (nM)	Fmut	Emax (%)	Basal (x induction)
WT-CCK2R	0.53 ± 0.12	1	1.61 ± 0.14	0.71 ± 0.21	1	100	1.12
H381A mutant	44.21 ± 2.65	83	1.64 ± 0.19	40.35 ± 0.15	56	51	1.10
Y385A mutant	47.52 ± 1.33	89	1.60 ± 0.15	42.35 ± 1.56	59	50	1.13
F110A mutant	0.72 ± 0.31	1.3	1.61 ± 0.30	0.57 ± 0.21	0.80	68	1.12
S137A mutant	0.94 ± 0.16	1.7	1.62 ± 0.09	0.92 ± 0.05	1.3	52	1.0
S131A mutant	1.15 ± 0.11	2.1	1.59 ± 0.12	0.98 ± 0.02	1.4	54	1.18
T193A mutant	1.01 ± 0.11	1.9	1.58 ± 0.15	1.02 ± 0.24	1.4	54	1.15
R158A mutant	0.58 ± 0.04	1.1	1.62 ± 0.21	0.51 ± 0.02	0.71	70	1.17
L330E mutant	0.11 ± 0.02	0.20	1.58 ± 0.25	0.09 ± 0.01	0.12	100	2.31
E151A mutant	0.09 ± 0.02	0.16	1.61 ± 0.10	0.08 ± 0.03	0.11	100	2.52

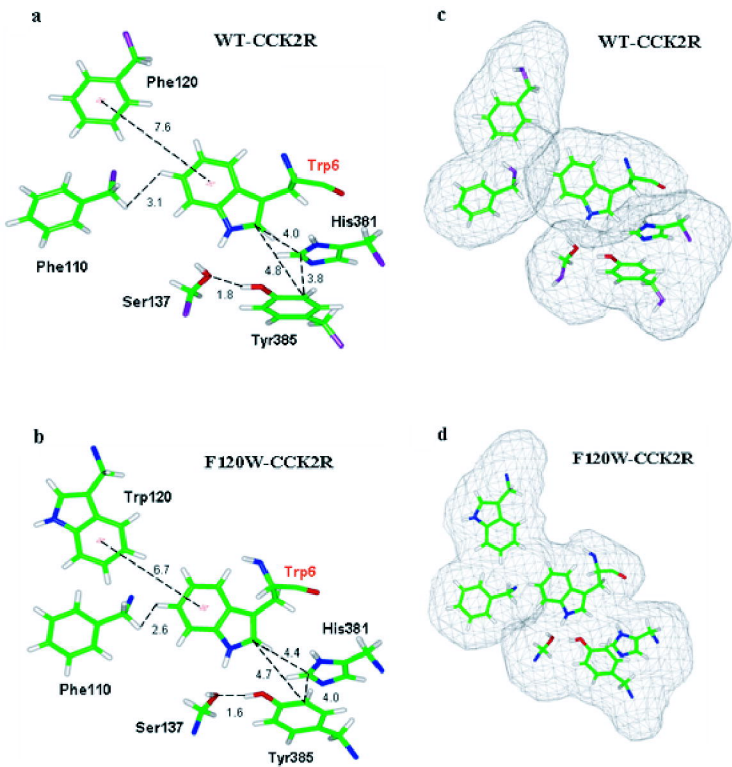


**FIGURE 1**

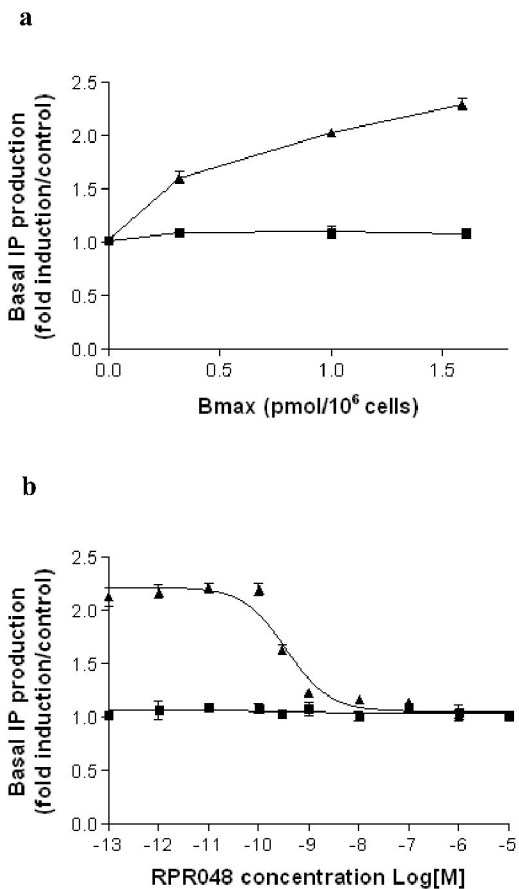
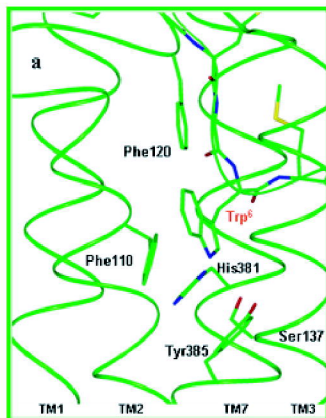
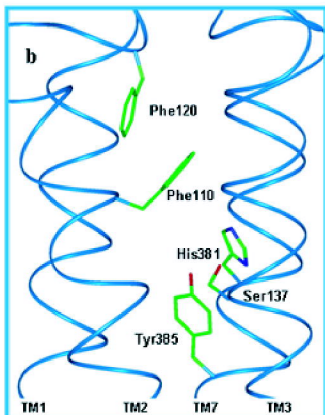


**FIGURE 2**

"Active model"



"Inactive model"



"Constitutively active F120W model"

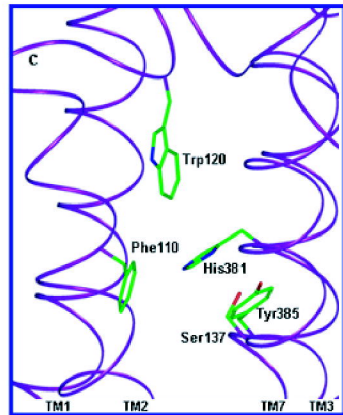
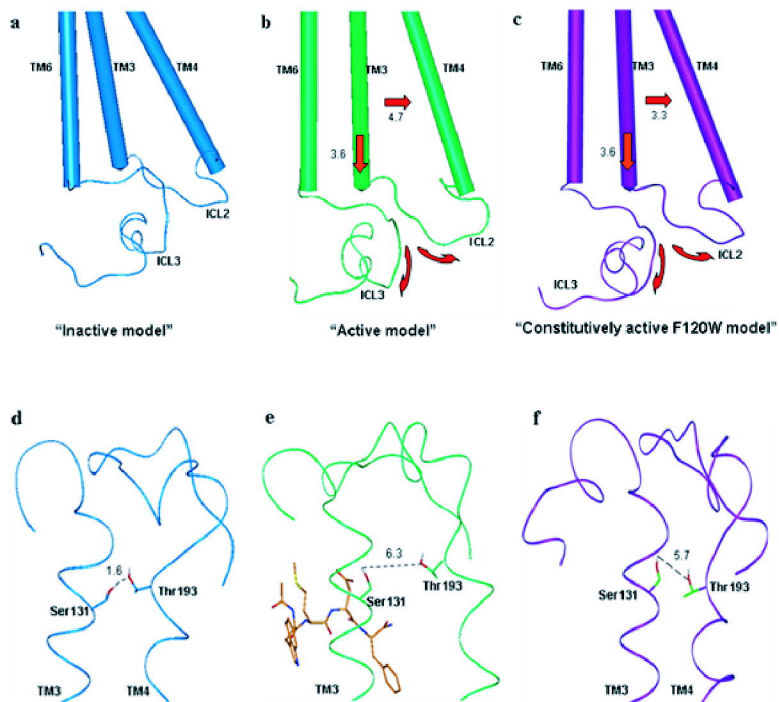
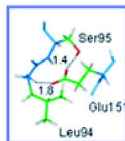
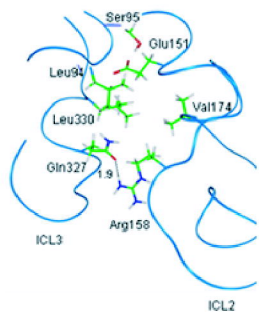
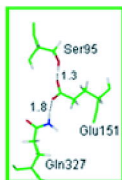
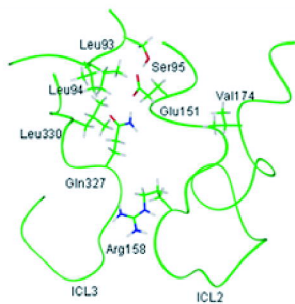
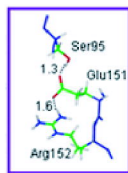
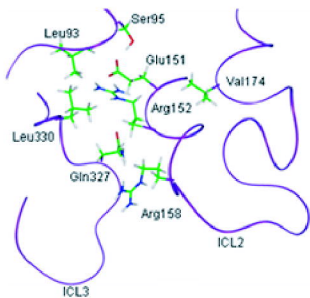


FIGURE 3



**FIGURE 4**

**a****b****c****FIGURE 5**